

A method for the determination of spatial electron density distribution in great Plasma-Focus devices

Andrzej Kasperczuk,
Marian Paduch,
Tadeusz Pisarczyk,
Krzysztof Tomaszewski

Abstract Determination of the electron density of plasma generated in a great plasma-focus device by means of interferometry is very difficult or sometimes impossible. In order to determine spatial electron density distributions of plasma in a PF-1000 device, a special method was prepared, with the use of plasma images obtained by means of both an optical frame camera and shadowgraphy. Analysis of plasma radiation in the very narrow $\Delta\lambda = 60 \text{ \AA}$ optical range allowed us to determine the relation between intensity of the plasma radiation and the electron density. It was also shown that the influence of electron temperature on plasma radiation is not large. The presented method allowed us to obtain spatial electron density distributions of plasma (in relative units) in the PF-1000 device. By means of this method a number of important information about the plasma-focus phenomenon was obtained.

Key words bremsstrahlung radiation • electron density distribution • frame optical camera • plasma-focus device • plasma radiation intensity • shadowgraphy

Introduction

One of the fundamental plasma parameters is the electron density. The knowledge of spatial electron density distributions during plasma evolution allows one to analyse a number of physical processes, such as: thermodynamic expansion of plasma, plasma-magnetic field interaction, flows and outflows of plasma, and MHD plasma instabilities. In order to obtain the electron density distribution, laser interferometry is usually used. This method was employed by the present authors in many experiments, also on plasma-focus devices [1–3, 5]. The main problem of the interferometric measurement is to obtain enough quality interferograms. The plasma generated in plasma-focus devices is still a very difficult object for investigation by means of the interferometric method. This is mainly due to:

- high frequency of interference fringes, above a spatial resolution of CCD cameras,
- high refraction of the probing laser beam.

In the case of very great plasma-focus devices, interferometric investigations are very difficult or sometimes impossible. This situation has occurred with the PF-1000 device, which is under investigation by the authors.

In order to obtain information about the spatial distribution of the electron density in the PF-1000 device, a special method was prepared. In this method plasma images obtained simultaneously by means of a frame optical camera and laser shadowgraphy are used instead of interferograms. This special method made it possible to obtain

A. Kasperczuk, M. Paduch, T. Pisarczyk✉, K. Tomaszewski
Institute of Plasma Physics and Laser Microfusion,
23 Hery Str., 00-908 Warsaw, Poland,
Tel.: +48 22/ 683 70 96, Fax: +48 22/ 666 83 72,
e-mail: pisaro@ifilm.waw.pl

Received: 18 June 2001

many interesting information about the plasma-focus phenomenon in the PF-1000 device. The investigations were carried out with deuterium as filling gas.

Physical bases of the presented method

In order to determine the electron density, the plasma radiation intensity recorded by means of the frame optical camera was used. Spectral range of the registered plasma light was limited to a very narrow range by means of an interference filter with the following parameters:

- maximum transmission for $\lambda = 5930 \text{ \AA}$,
- transmission window $\Delta\lambda = 60 \text{ \AA}$.

The position of the spectral window allowed to avoid the line radiation of plasma and impurities. Therefore, it could be assumed that the camera recorded only continuous radiation (recombination and bremsstrahlung). The results of previous investigations allowed us to assume also that the tested plasma during the final phases of a discharge fulfilled the LTE condition for the electron density, which in the analysed case is expressed by the formula [6]:

$$(1) \quad n_e \geq 2.52 \times 10^{17} T_e^{1/2}$$

where: n_e – electron density in cm^{-3} , T_e – electron temperature in eV.

Due to the narrow band of the applied spectral window, the equations describing the recombination (ϵ^{rb}) and bremsstrahlung (ϵ^{fb}) emission coefficients [4] are practically independent on the wavelength and become more convenient for analysis.

Next, it was proved, that the ratio

$$(2) \quad \frac{\epsilon^{rb}}{\epsilon^{fb}} \ll 1$$

in the considered range of plasma parameters. Although this ratio depends only on the electron temperature of plasma, it is a very complex function. Therefore it was counted by means of a numerical procedure. The Gaunt factors were taken from [7]. The results of computation are shown in Fig. 1. The diagram indicates that for $T_e > 20 \text{ eV}$ the recombination radiation can be neglected. The results of earlier investigations and computer modelling of the plas-

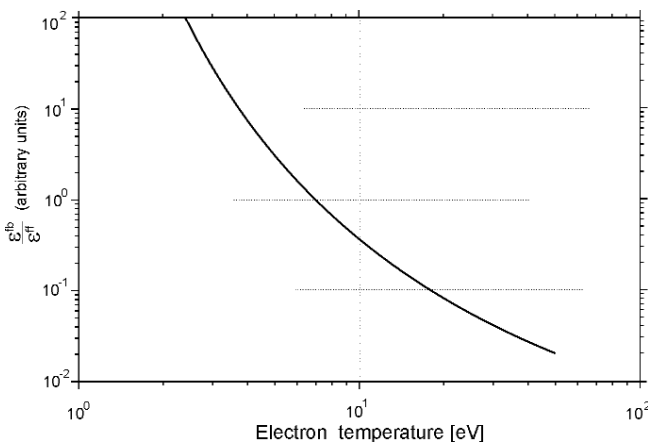


Fig. 1. Ratio of the recombination (ϵ^{rb}) and bremsstrahlung (ϵ^{fb}) emission coefficients as a function of electron temperature.

ma-focus phenomenon show that the electron temperature of the compressed plasma inside both the plasma sheath and the plasma column fulfills this condition. Therefore, only the bremsstrahlung radiation is taken into account in subsequent considerations. The final form of the emission coefficient of the bremsstrahlung radiation is expressed by the formula:

$$(3) \quad \epsilon^{fb} = 4.31 \times 10^{-37} \frac{n_e^2}{T_e^{0.307}} \exp\left(\frac{-2.09}{T_e}\right),$$

where: n_e in cm^{-3} , and T_e in eV.

The relative values of this coefficient as a function of n_e (diagram a) and T_e (diagram b) are presented in Fig. 2. One may see that ϵ^{fb} strongly depends on n_e , but its dependence on T_e is of little consequence. Therefore, the influence of T_e on ϵ^{fb} can be neglected and ϵ^{fb} is treated as a function of n_e only. If a photocathode of the camera works in the linear range, then the recorded plasma radiation intensity I is proportional to ϵ^{fb} , so I is proportional to n_e^2 .

Determination of the spatial electron density distribution

The determination of the spatial electron density distribution must take into account the axial symmetry of the tested plasma. Thus, images from the camera (Fig. 3a) are transformed by the known Abel equation. The actual distribution of the plasma radiation intensity $I(r, z)$ is shown in Fig. 3b. Because $I \sim n_e^2$, therefore the electron density distribution can be obtained by extracting the root of the numerical

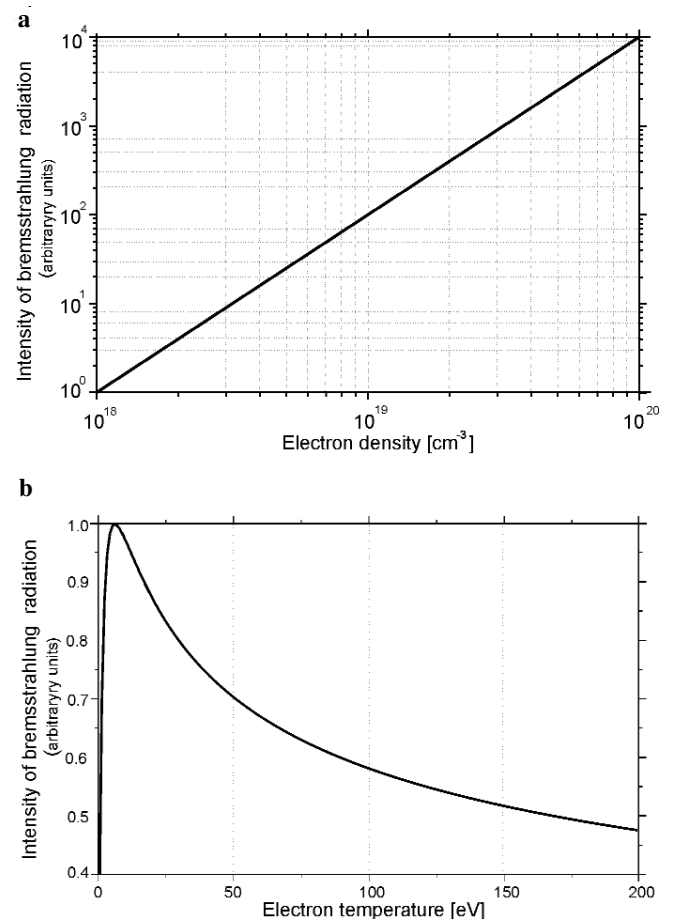


Fig. 2. Dependence of the bremsstrahlung radiation on electron density (a), and electron temperature (b).

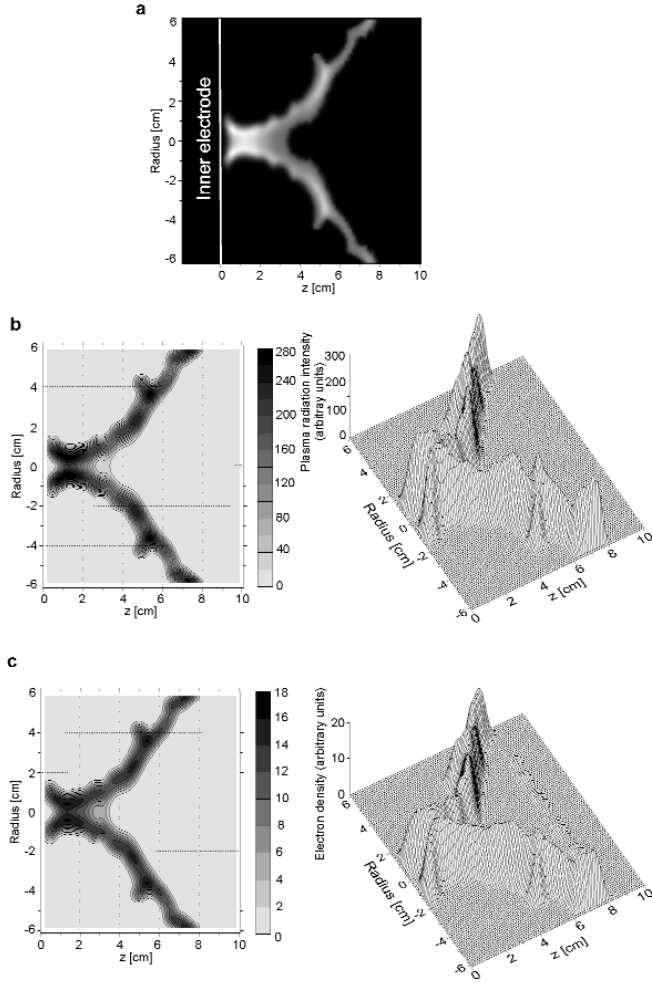


Fig. 3. Treatment of the electron density distribution determination: a – the plasma picture, b – the plasma radiation intensity distribution after the Abel transformation, c – the electron density distribution.

distribution of I . It must be pointed out that the n_e distribution (Fig. 3c) has a relative character, but for many analyses this kind of the n_e distribution is sufficient.

Because the electron temperature is not considered in this computation, so the influence of T_e is treated as an error of n_e values. It is estimated that this error is less than 30%. Since the plasma radiation intensity depends mainly on n_e , therefore, determination of the plasma boundary, where n_e may be very low, is sometimes impossible. Information about the plasma boundary is important from two reasons:

- allows to determine actual sizes and shape of plasma,
- determines integration limits in the Abel transformation.

To determine the plasma boundary, the laser shadowgraphy is very useful. The two following phenomena constitute the basis of the shadowgraphy measurement on plasma-focus devices:

- deflection of laser rays due to gradients of the electron density,
- occurrence of the maximum gradient at the plasma boundary due to magnetic field pressure.

The propagation of a laser ray through the axially symmetrical non-homogeneous plasma is demonstrated in Fig. 4. Due to the component of the n_e gradient perpendicular to the direction of a ray propagation, the ray undergoes deflection by an angle described by the following formula:

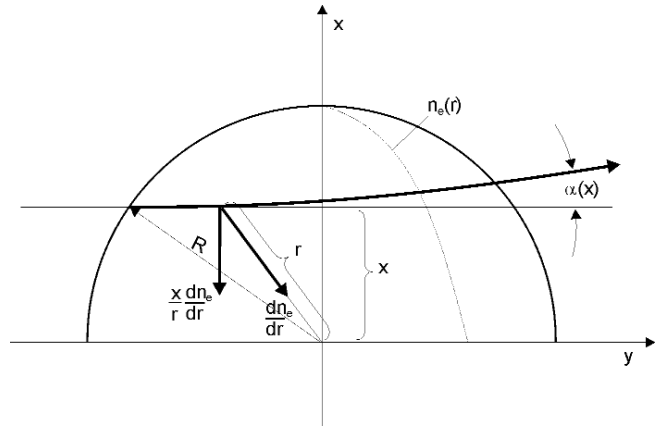


Fig. 4. Illustration of the light ray propagation through in homogeneous plasma.

$$(4) \quad \alpha(x) = \frac{1}{n_c} \int_x^R \frac{x}{r} \frac{dn_e}{dr} (r^2 - x^2)^{-1/2} r dr,$$

where:

$$(5) \quad n_e = 1.12 \times 10^{13} \lambda^{-2}$$

λ – the wavelength of laser radiation in cm.

To register the plasma boundary, a very simple optical system is used. This system consists of two elements: a lens and a diaphragm (Fig. 5). If the diaphragm has a relatively large diameter, only the most deflected rays are stopped, but when its diameter is decreased little by little, then less deflected rays are gradually stopped. Therefore, the diameter of the diaphragm influences the width of the registered plasma contour. To illustrate this influence, it was assumed that the profile of $n_e(\rho)$, where $\rho = x/R$, is described by the following parabolic form:

$$(6) \quad n_e(\rho) = n_{e\max}(1 - \rho^2),$$

with a maximum electron density of 10^{19} cm^{-3} (see Fig. 6). This profile results in the distribution of the deflection angle, $\alpha(\rho)$, expressed by the formula:

$$(7) \quad \alpha(\rho) = \frac{2n_{e\max}}{n_c} \rho \sqrt{1 - \rho^2} = 0.02 \rho \sqrt{1 - \rho^2} \quad [\text{rad}]$$

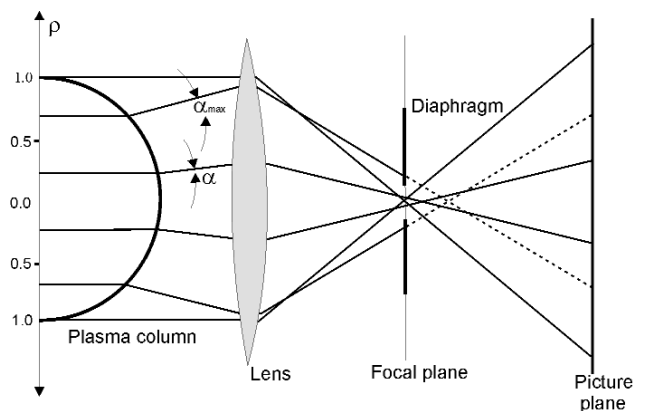


Fig. 5. Scheme of the shadowgram registration of axial symmetrical plasma; dashed lines behind the diaphragm denote rays stopped by diaphragm.

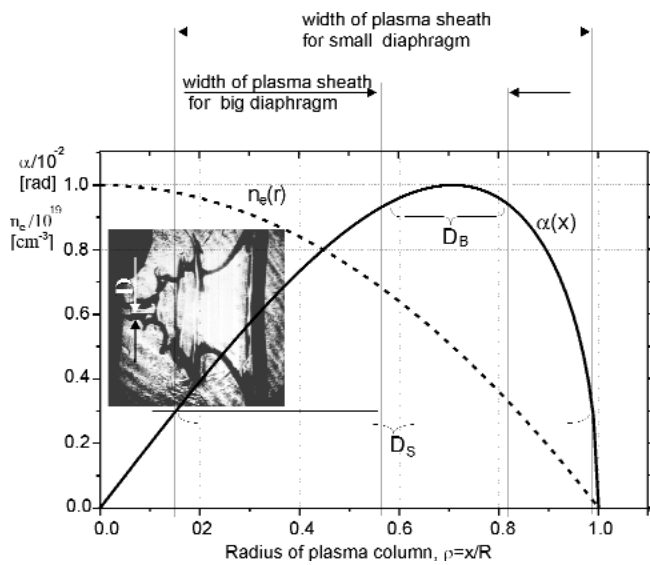


Fig. 6. Influence of the parabolic plasma distribution on laser beam diffraction.

D_B and D_S in Fig. 6 are the widths of the plasma contour for the large and small diaphragms, respectively. It is obvious that more precise reconstruction of the plasma boundary occurs in the case of the small diaphragm.

The shadowgraphy is an auxiliary method in the course of determination of the n_e distribution. This method is employed when plasma images from the optical camera and shadowgraphy differ considerably. The images in Fig. 7a correspond to the maximum plasma compression state ($t=0$). Up to this moment, the images from both diagnostics are compatible. Essential differences appear for the later time. The image from the camera in Fig. 7b suggests that the radius of the plasma column decreased during last 50 ns, while in fact an expansion of the plasma column occurs (compare shadowgrams in Figs. 7a and 7b). So, only analysis of both plasma images gives a proper information about the processes occurring in the plasma-focus phenomenon.

Conclusions

A special method for the determination of the electron density distribution was prepared, particularly for the PF-1000 experiment. Due to the great scale of the PF-1000 device, no traditional method could be used. In spite of the limitations of this method, such as: a comparatively great error of the electron density determination and the relative scale of the electron density distribution, thanks to it many information about plasma produced in the great plasma-focus device were obtained [4]. On this account, an increasing role of the high-speed frame optical cameras for investigations of the plasma-focus phenomena is of interest. The

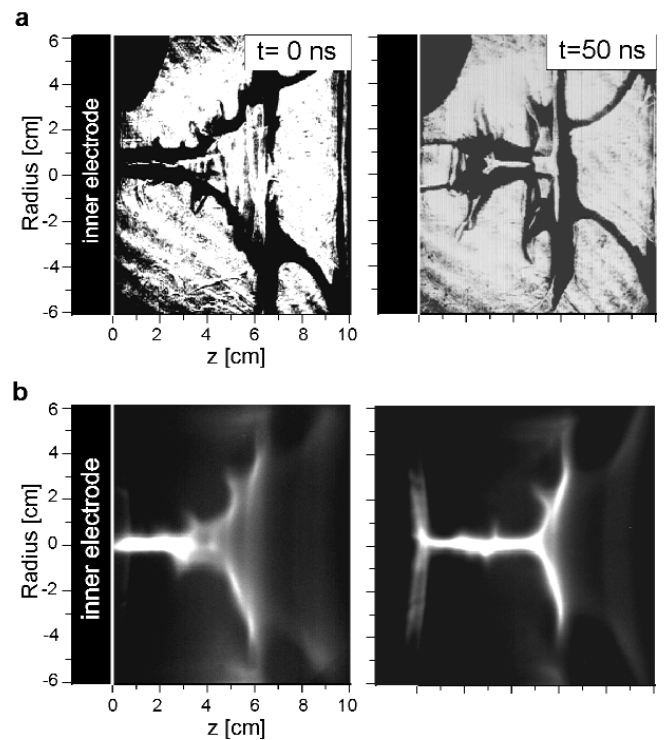


Fig. 7. Images of plasma from shadowgraphy (a) and the optical camera (b) for two different moments of the plasma-focus phenomenon.

cameras, which have been aimed at a plasma configuration visualization, become a more universal research tool.

References

1. Czekaj S, Denus S, Kasperczuk A, Miklaszewski R, Paduch M, Pisarczyk T, Wereszczyński Z (1985) MHD stability of plasma in the PF-150 device. In: Proc of the 4th Int Workshop on Plasma Focus and Z-pinch Research. Warsaw, Poland 1:124–127
2. Czekaj S, Denus S, Kasperczuk *et al.* (1983) Evolution of plasma column and its connection with neutron emission in the plasma-focus PF-150 device. In: Proc 11th Eur Conf on Controlled Fusion and Plasma Physics. Aachen, Germany 1:469–473
3. Czekaj S, Kasperczuk A, Miklaszewski R, Paduch M, Pisarczyk T, Wereszczyński Z (1989) Diagnostic method for the magnetic field measurement in plasma focus device. *Plasma Phys Contr Fusion* 31;4:587–594
4. Kasperczuk A, Kumar R, Miklaszewski R, Paduch M, Pisarczyk T, Tomaszewski K, Scholz M (2002) Study of the plasma evolution in the PF-1000 device by means of optical diagnostic. *Phys Scripta* 65:96–102
5. Kasperczuk A, Pisarczyk T (1996) Interferometric investigations of laser-produced plasma in strong external magnetic field. *Phys Scripta* 53:503–507
6. Lochte-Holtgreven B (ed) (1970) *Plasma diagnostics*. North-Holland Pub. Co., Amsterdam
7. Rosenbluth MN, Sagdeev RZ (eds) (1983) *Hand-book of plasma physics*, vol. 1. North-Holland Pub. Co., Amsterdam